TWELFTH EUROPEAN ROTORCRAFT FORUM

Paper No. 70

STRUCTURAL ANALYSIS AND DESIGN CONSIDERATIONS OF ELASTOMERIC DAMPERS WITH VISCOELASTIC MATERIAL BEHAVIOR

Gerhard Hausmann

Messerschmitt-Bölkow-Blohm GmbH
München, F.R.G.

September 22-25,1986
Garmisch-Partenkirchen
Federal Republik of Germany

STRUCTURAL ANALYSIS AND DESIGN CONSIDERATIONS OF ELASTOMERIC DAMPERS WITH VISCOELASTIC MATERIAL BEHAVIOR

Gerhard Hausmann

Messerschmitt-Bölkow-Blohm GmbH
München, F.R.G.

Abstract

At present, a new generation of high-performance elastomeric materials is introduced in modern rotor systems.
The field of application ranges from low damping elastomers for layered high-capacity elastomeric bearings to high damping elastomers for lead-lag dampers. All such materials show a significant nonlinear and almost incompressible material behaviour, which can be described in the static range by hyper-elastic material models and in the dynamic range by viscoelastic constitutive equations. Ultimate values and dynamic mechanical properties are highly dependent on parameters such as frequency, temperature, amplitude and pre-load. In addition mechanical property changes are due to aging and dynamic fatigue.

An optimized structural design for the whole range of application, requires a solid knowledge of the mechanical material characteristics. This paper describes some representative results of the theoretical and experimental work which is done at MBB in developing viscoelastic lead-lag-damper in bearingless main rotor systems.

1. General Outlines

High damping elastomeric materials with profound viscoelastic material behavior find increasing application in the modern helicopter design. The basic principle lies in the fact of the conversion of kinetic energy into internal heat by hysteresis effects. By use of such elastomers in the lead-lag damping of bearingless rotors, natural in-plane frequencies, damping behavior and thus, the stability of the rotor system (ground and air resonance) are deceisively influenced by the material properties and damper design. The successfull application of elastomeric dampers depends to a great deal on the following important factors:

- Exact knowledge of structural dynamics of the considered rotor system
- Properties of the damper materials at various environmental and load conditions
- Optimized damper design for following requirements

  - o static and dynamic spring rates
  - o rate of dissipation
  - o lifetime
  - o compression set
  - o damper stability etc.

under consideration of permissible values of strength and heat built-up. The material properties are highly nonlinear dependent on the outer parameters such as load, temperature, frequency and service time, therefore, the sensitivity of this material in view to the given environmental conditions must be critically examined during the design phase. For providing such information, a thorough knowledge about the properties of the applied elastomers is necessary.

Since stiffness, damping and strength behavior are not constant over a wide range of load and environmental conditions, the dampers are optimized for the point with the highest probability of occurence (design point) under consideration of permissible strains, maximum loss factor (versus strain) and required dynamic spring rates.

2. Notes on the Design Principles of Lead-Lag Dampers in Bearingless Soft-Inplane Rotors

The lead-lag damping concept for a bearingless rotor system, presented in figure 1.1, has eight discrete pair-like arranged viscoelastic lead-lag dampers. As shown in figure 2, a periodic in-plane motion of the rotor blade about the lead-lag hinge causes on the point of damper installation a relative displacement between flexbeam and cuff. The resulting shear deformation of the bonded elastomeric material produces the damping forces and corresponding dissipation energy to prevent air or ground resonance of the considered rotor system. The conversion of kinetic lead-lag energy into internal heat is a direct function of damper shear displacements (or shear forces) and the corresponding frequencies.

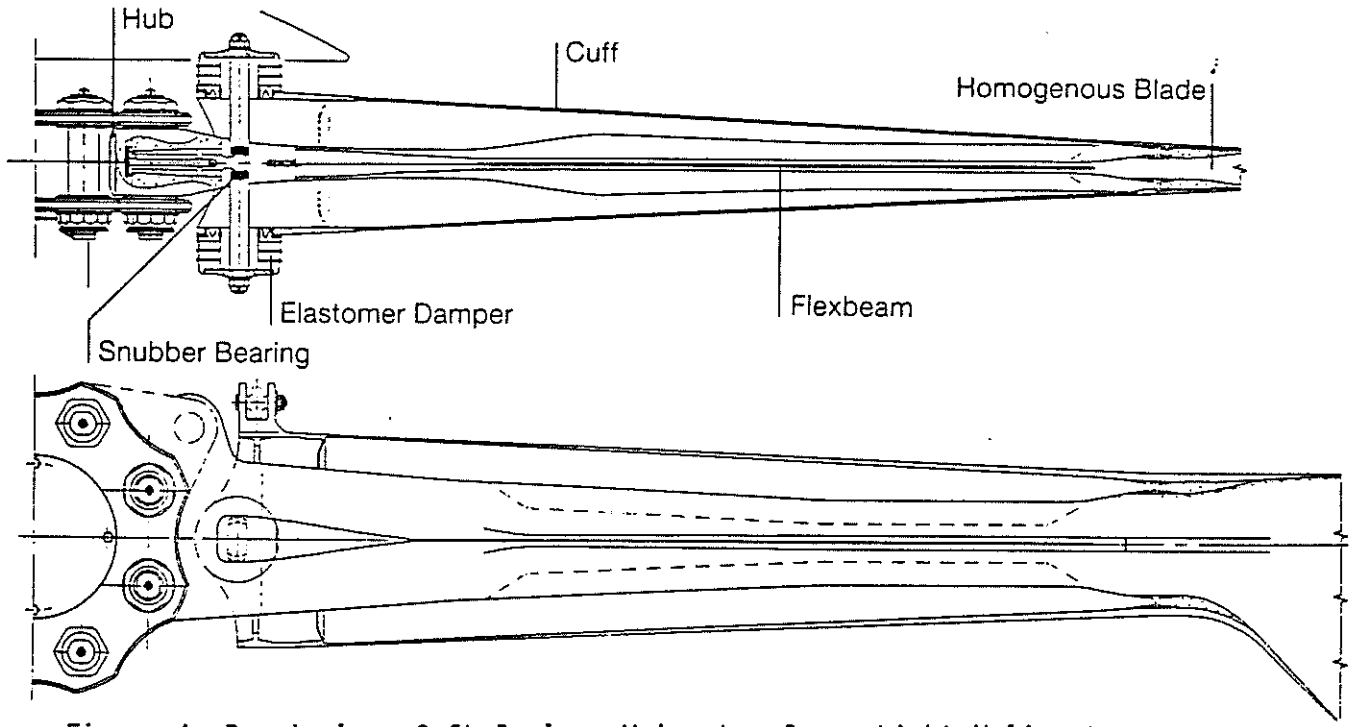

Figure 1: Bearingless Soft-Inplane Mainrotor for a Light Helicopter

An optimized damper design requires therefore an appropriate tuning of dynamic characteristics of blade, cuff and dampers under consideration of maximum loss power, load and environmental conditions, damper stability and acceptable operating stress and strain values.

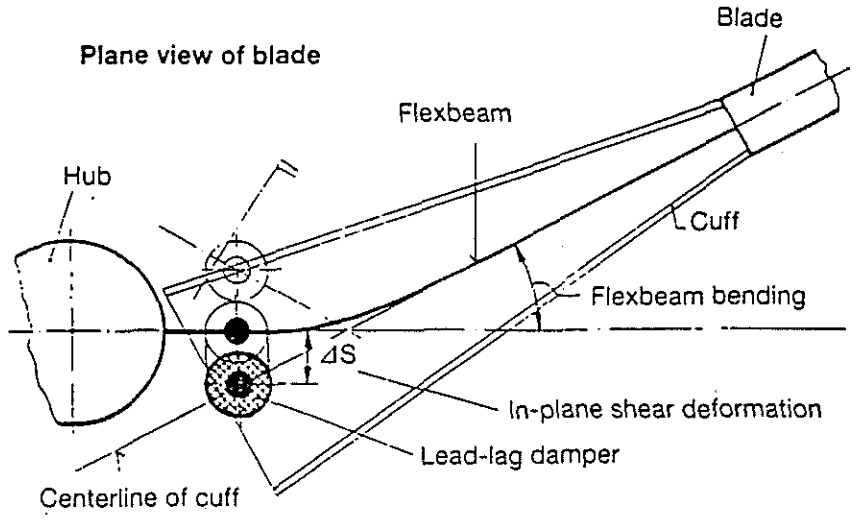

Figure 2: Principle sketch of Lead-Lag Damper and Inplane Blade Kinematic

3. Design Parameters

The large number and the complicated dependence of the influence factors is characteristic for all problems with which we are confronted in the design of high damping elastomers. The possibility to describe the most important influence factors plays a deceisive role in damper optimization and rotor system tuning. Some important design parameters can be summarized as follows:

o Material Point of View

- Hyperelastic and viscoelastic material properties
- Drift characteristic
- Thermodynamic properties, heat build-up characteristic
- Permissible stresses and strains
- Bond strength etc.

o Damper Point of View

- Companion dimensions, elastic stops, weight
- Static and dynamic lateral and axial spring rates, working range
- Dissipation rate, temperature distribution, low temperature stiffening
- Stress and strain distribution
- Lifetime, strength and stability at combined loads
- Compression relaxation, axial preload

o Rotorsystem Point of View

- Rotor geometry and kinematic, structural damping, weight
- Ground and air resonance stability bounds, coupling effects
- Static and dynamic characteristic of blade and cuff system
- Load and motion spectrum,limit loads, permissible strength values
- Natural lead-lag frequencies and blade damping as a function of damper characteristic
- Appropriate tuning of the system blade-cuff-damper under consideration of the total load spectrum and the given wide range of environmental conditions
- Optimal working range and therefore the required range of damper, spring rate and loss factor

4. Optimization Steps

There are two main steps in the preliminary damping optimization stage:

A) Optimization of rotor system damping (lead-lag damping) by means of an appropriate tuning of blade, cuff and damper.

B) Optimization of the discrete viscoelastic damper corresponding to the results of the first step and other technical requirements.

A suitable design diagram for the first optimization step is shown in figure 3. This diagram represents the variation of the first lead-lag frequency (ω_ζ) and modal blade damping (D_ζ) with respect to the elastic damper spring rate (K'). The ideal linear viscoelastic material is modelled as an equivalent viscous damping coefficient, which provides the same energy dissipation (N_{Diss}) and dynamic spring rate (K*, K') as the elastomeric damper (2-parameter model).
There is no difference between the viscose and the elastomer damper at a constant frequency with respect to the dynamic behavior.

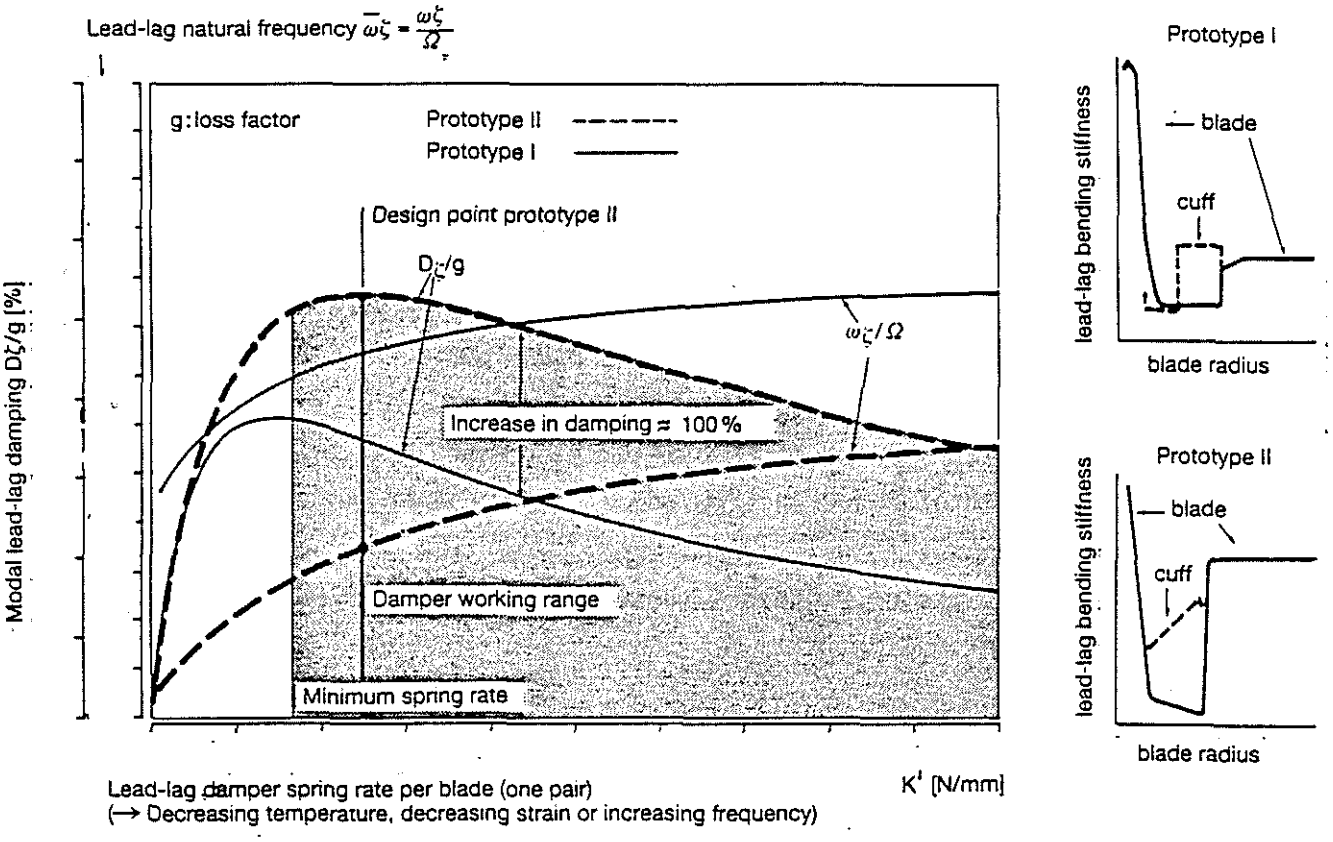

Figure 3: Modal Lead-lag Damping and Lead-Lag Natural Frequency as a Function of Elastic Damper Spring Rate

As far as stability boundaries of the rotor system are concerned, the predesign diagram of figure 3 provides the required damper characteristic, such as the appropriate range of spring rate and damping (loss power). It is important to note that damper loss factor and stiffness vary highly with temperature, strain and axial precompression.

With respect to the divergent design goals, such as spring rates, damping and lifetime, the optimization procedure requires a thorough knowledge of all influence parameters.

In the following, priority is given to the second preliminary design step, especially to the basic questions of material and damper characteristics.

5. Stiffness and Dissipation Characteristics of Elastomer Dampers

5.1 Basic Principle

In general, the stiffness characteristic of elastomer dampers depends on the static preload, dynamic amplitude, frequency, temperature etc. A typical load-deflection curve for an arbitrary load direction is given in figure 4.

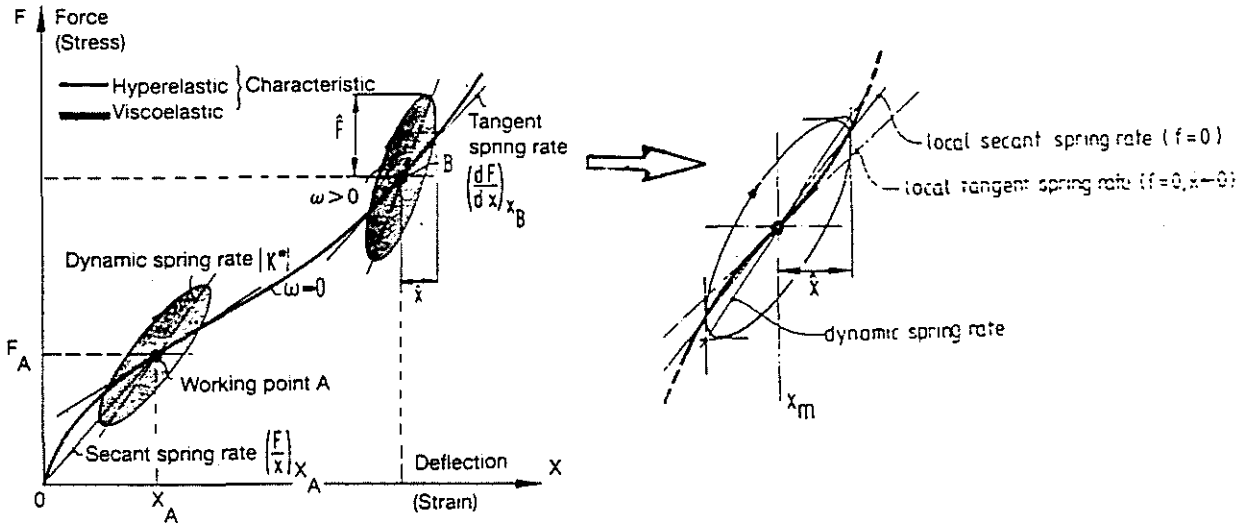

Figure 4: Spring Rate Characteristic of Elastomer Damper

The static work points (mid loads or deflections) are represented by the nonlinear elastic equilibrium curve. The complete static curve is described by the secant stiffness $K_{S,A} = (F/X)_A$; the tangent stiffness $K_{T,A} = (dF/dx)_A$ represents the linearised spring rate in the vicinity of a nonlinear prestrained state.

In the case of periodic loading, a viscoelastic hysteresis loop is superposed to the equilibrium curve at the working point. The resulting absolute dynamic spring rate is defined by $|K^*| = \hat{F}/\hat{x}$ with $\hat{F}$ and $\hat{x}$ as the dynamic load and deflection amplitude, respectively. $|K^*|$ is always greater than the corresponding tangent spring rate and increases with an increase in frequency. The hysteretic loops can be represented as a combination of different material properties, such as hyperelasticity and viscoelasticity.
Figure 5 shows the linear and nonlinear individual elements of the dynamic characteristic of the damper and two derived hysteretic loops.

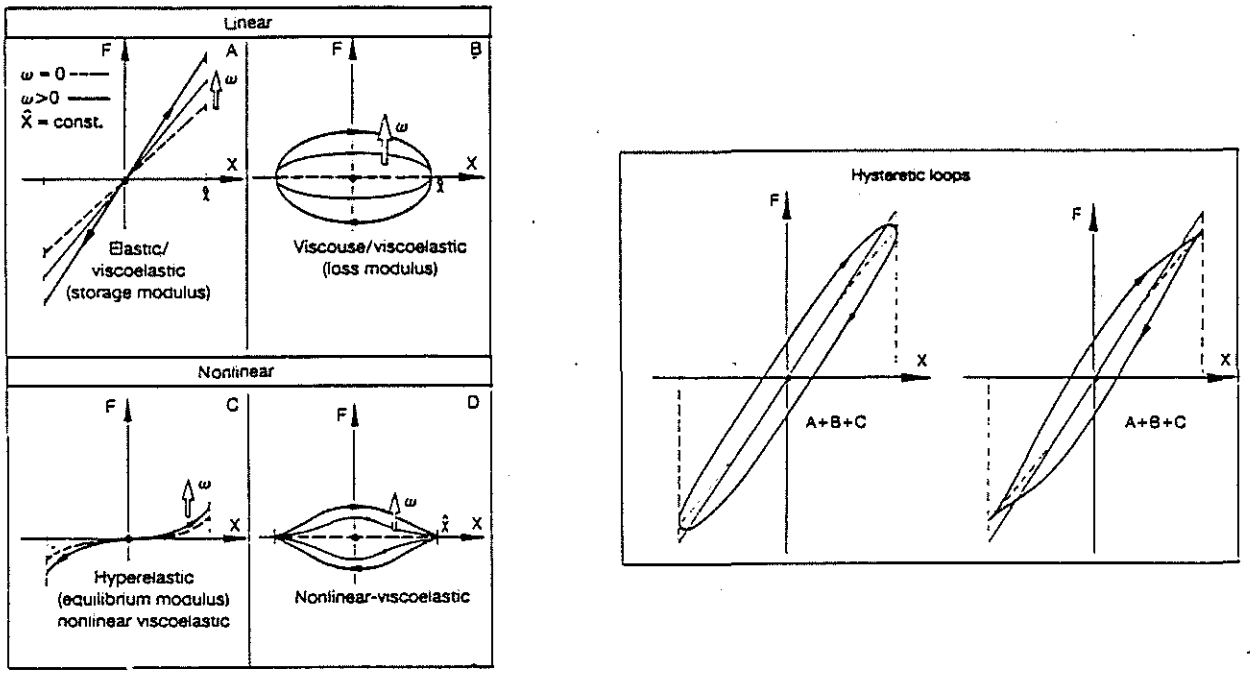

Figure 5: Hyperelastic and Viscoelastic Elements of a Nonlinear Hysteresis Loop

5.2 Static Spring Rate

Linearisation of the hyperelastic equilibrium curve at a given working point (A) provides the differential spring rate K for the selected load direction. The linearized static tangent stiffness matrix for a typical damper as shown in figure 6, can be expressed by

$$\begin{bmatrix} F_1 \\ F_2 \\ F_3 \\ \hline M_4 \\ M_5 \\ M_6 \end{bmatrix} = \left[\begin{array}{ccc:ccc} K_{11} & 0 & 0 & 0 & 0 & 0 \\ 0 & K_{22} & 0 & 0 & 0 & K_{26} \\ 0 & 0 & K_{33} & 0 & K_{35} & 0 \\ \hdashline 0 & 0 & 0 & K_{44} & 0 & 0 \\ 0 & 0 & K_{53} & 0 & K_{55} & 0 \\ 0 & K_{62} & 0 & 0 & 0 & K_{66} \end{array}\right] \cdot \begin{bmatrix} X_1 \\ X_2 \\ X_3 \\ \hline \varphi_4 \\ \varphi_5 \\ \varphi_6 \end{bmatrix}$$

, where

Loads — static tangential stiffness matrix — Deflections

axial spring rate : K_{11} ; torsional spring rate: K_{44}

lateral spring rates: K_{22}, K_{33} ; cocking spring rate : K_{55}, K_{66}

couple terms : K_{26}, K_{62}; K_{53}, K_{35}.

or, in short, $\underline{F} = \underline{\underline{K}}_A \cdot \underline{X}$

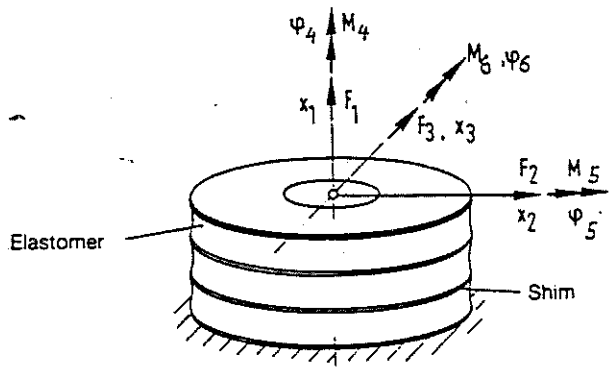

Figure 6: Coordinate System of a Typical Multiaxial Loaded Elastomer Damper

The static components K_{ij} depend on preload (rsp. predeflection) and temperature: $K_{ij} = K_{ij}\ (X_m, \vartheta)$.

5.3 Dynamic Spring Rate and Definition of Damping

The dynamic spring rate is defined by the shape of the measured hysteretic loop at a given working point. A typical test arrangement for dynamic stress or strain controlled shear tests at low frequencies (0 ... 20 Hz) is shown in figure 7; test parameters are frequency, amplitude, predeflection, axial compression and temperature. The measured hysteresis loop gives important information on the dynamic damper characteristics for the steady state cyclic behavior [1].
In this case, two different suitable methods are used to describe the damper behavior: the mathematical and the physical modelling.

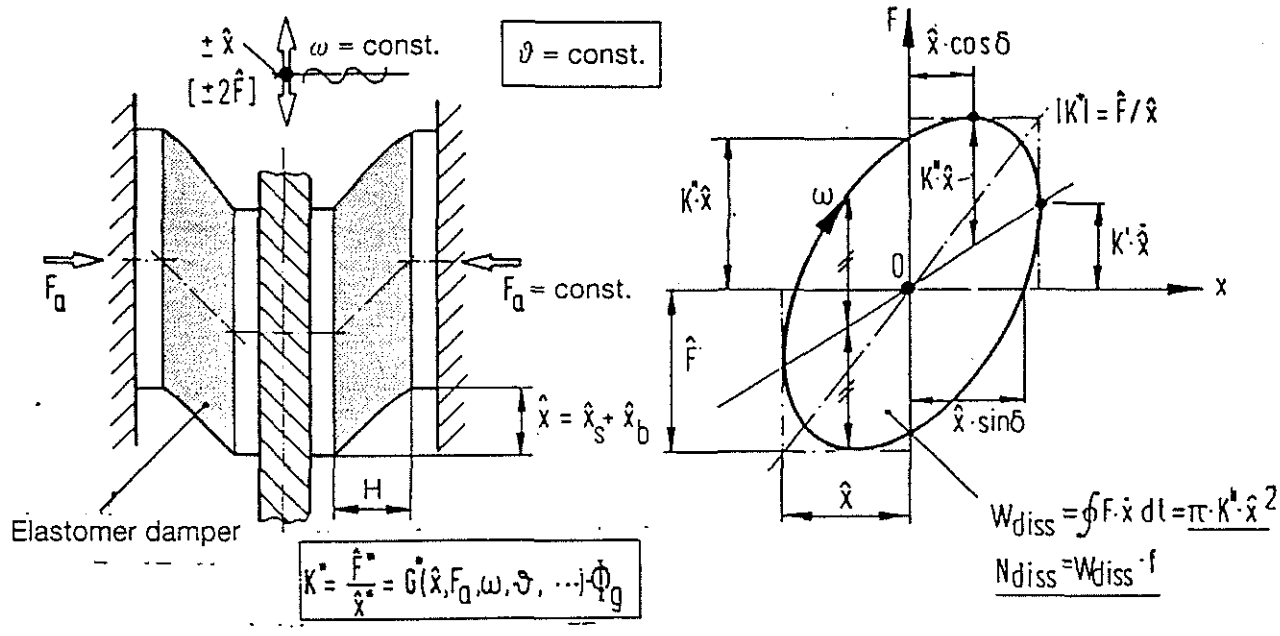

Figure 7: Dynamic Shear Test of Bonded Elastomer Dampers

The hysteresis loop is a representation of steady state periodic behavior. The corresponding damper characteristic for strong nonlinear elliptic hysteresis loops can be written mathematically in a general force-displacement law (without inertial forces):

$$F(\vec{x}) = K_0 \vec{x} + \phi_1(\vec{x})$$
$$F(\overleftarrow{x}) = K_0 \overleftarrow{x} - \phi_2(\overleftarrow{x})$$

This pair of equations, which occupies different parts of the time-domain, can approximately be solved by the method of the Harmonic Balance (phase plane analysis). Figure 8 shows measured hysteresis loops with different amplitudes and their mathematical approximation (dotted lines).

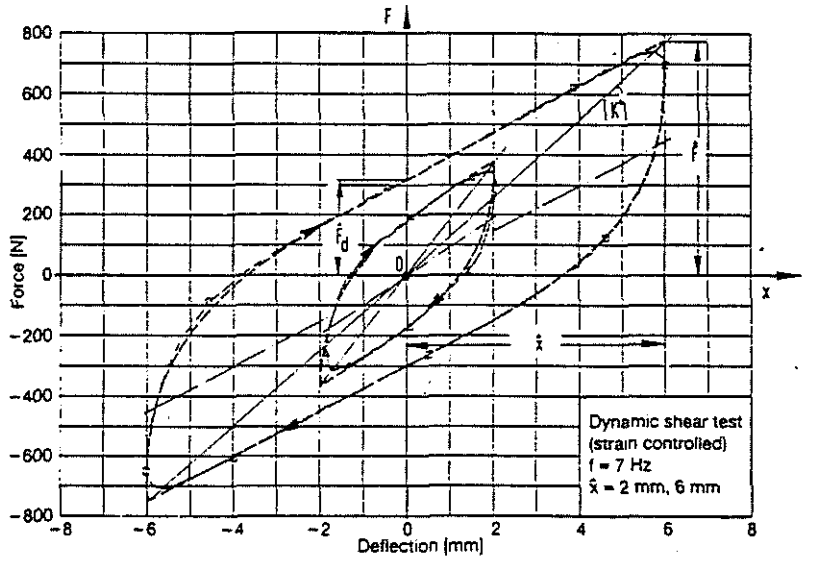

Figure 8: Direct Mathematical Description of Nonlinear Hysteretic Loops

Physical models of dampers are based on the description of the measured material behavior with appropriate constitutive equations. In the damper characterization we have to differentiate between conservative (hyperelastic) effects and dissipative (viscoelastic) effects. Hyperelastic constitutive equations are represented by a strain energy potential function W. Viscoelastic material properties are given by the equilibrium constants and an appropriate dissipation function $\mathbf{H}^*$.

In the frequency domain, the cyclic spring rate characteristic of visco-elastic dampers can be suitably described by the complex modulus approach, see figure 9.

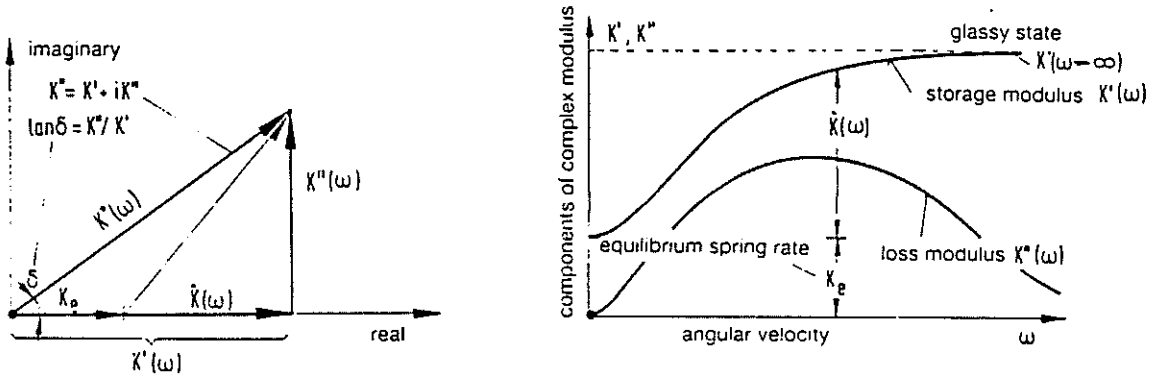

Figure 9: Vector Diagram for Complex Modulus and the Effect of Frequency on the Dynamic Damper Characteristic

Generally, the complex spring rate is defined as

$$K^*(i\omega) = F^*/x^* = K' + iK'' = K_e + \mathbf{H}^*(i\omega)$$

where K_e: equilibrium modulus; $\mathbf{H}^*=\mathbf{H}^*(i\omega)$: dissipation function.
In case of multiaxial periodic loadings the damper characteristic can be written in an appropriate complex form:

$$\underline{F}^* = \underline{\underline{K}}_A^* \cdot \underline{X}^*$$

where $\underline{F}^*$: complex force vector, $\underline{X}^*$: complex displacement vector and $\underline{\underline{K}}^*_A = \underline{\underline{K}}'_A + i\cdot\underline{\underline{K}}''_A$: complex stiffness matrix.
Based on the traced hysteresis loop the dynamic spring rate $|K^*| = \hat{F}/\hat{x}$ and the damping parameters are determined. There are two fundamental definitions of the mechanical loss factor $\tan\delta$.

The first definition is given by

$$\delta = \sin^{-1}\left(\frac{A_{diss}}{\pi \cdot \hat{F} \cdot \hat{x}}\right), \text{ where } A_{diss} = \oint F dx = \int_0^{2\pi/\omega} F \dot{x}\, dt$$

and $\hat{F}$: maximum load; $\hat{x}$: maximum deflection; δ: loss angle

The second definition is given by

$$\delta = \tan^{-1}\left(\frac{A_{diss}}{2 \cdot \pi \cdot U_s}\right), \text{ where the strain energy } U_s = \frac{1}{2} K' \hat{x}^2 \text{ is}$$

represented in figure 10 of the area 0-1-2-3-0.
The determination of strain energy by an nonlinear-elastic "mid-force" curve

$U_{s,mid} = \oint F_{mid}\, dx$ (area 0-4-2-3-0) has the disadvantage of inconsistence together with the other viscoelastic relations.
The mechanical loss factor $\tan\delta$ and therefore all related parameters are dependent on shape factor, amplitude, frequency and temperature. It is noted that $\tan\delta$ and Λ/π can diverge markedly, (Λ = logarithmic decrement).

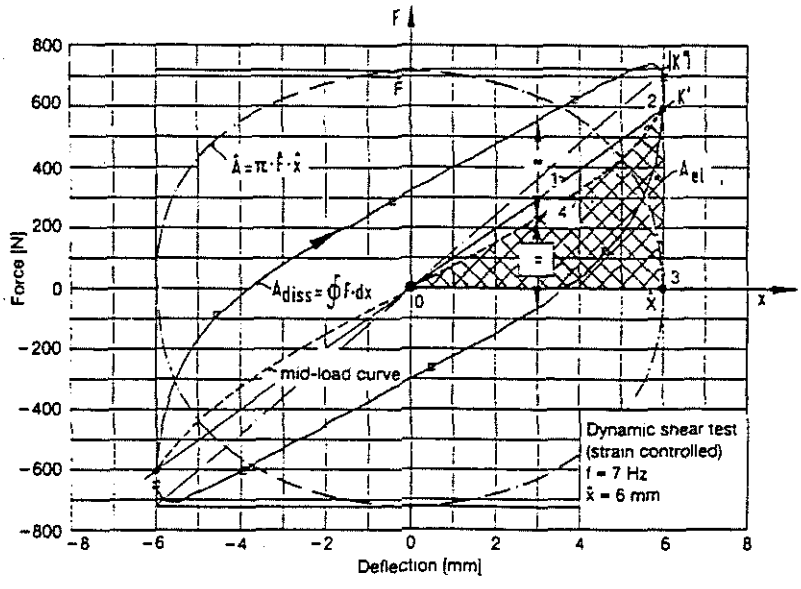

Figure 10: Definition of Damping in Terms of Hysteretic Loop

For the description of real damper properties by the methods of visco-elasticity, nonlinear hysteresis loops are suitably linearized.
The dynamic spring rate $|K^*|$ and the loss factor $\tan\delta$ in the two types of loops are constant.
Figure 11 represents this linearization by an elliptical loop.

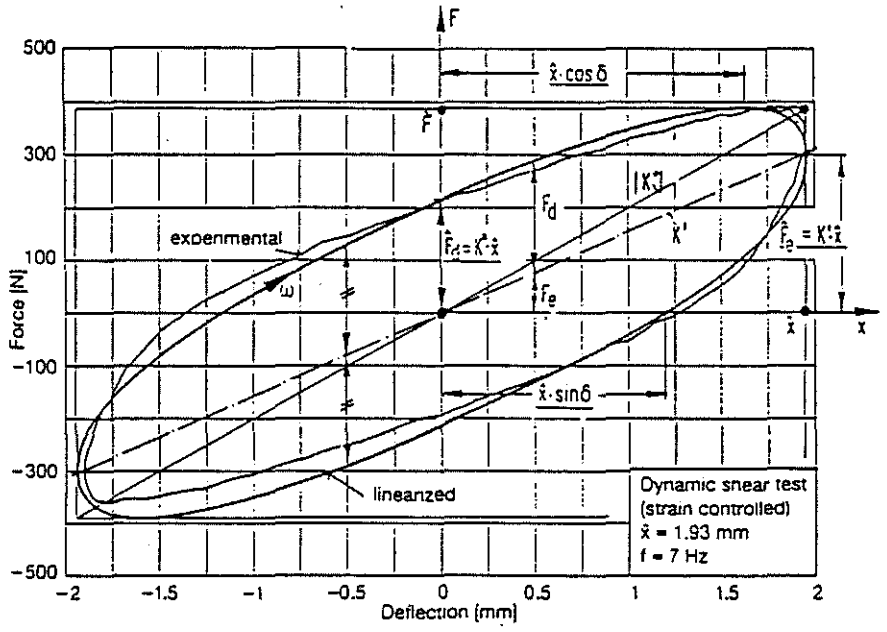

Figure 11: Linearization of a Nonlinear Hysteresis Loop
(Equivalent Damping Method)

The main influence parameters on shear stiffness and loss coefficient are amplitude, frequency, temperature and axial compression. Figure 12 represents qualitatively the performance graphs for stiffness and damping in dependence on these parameters.

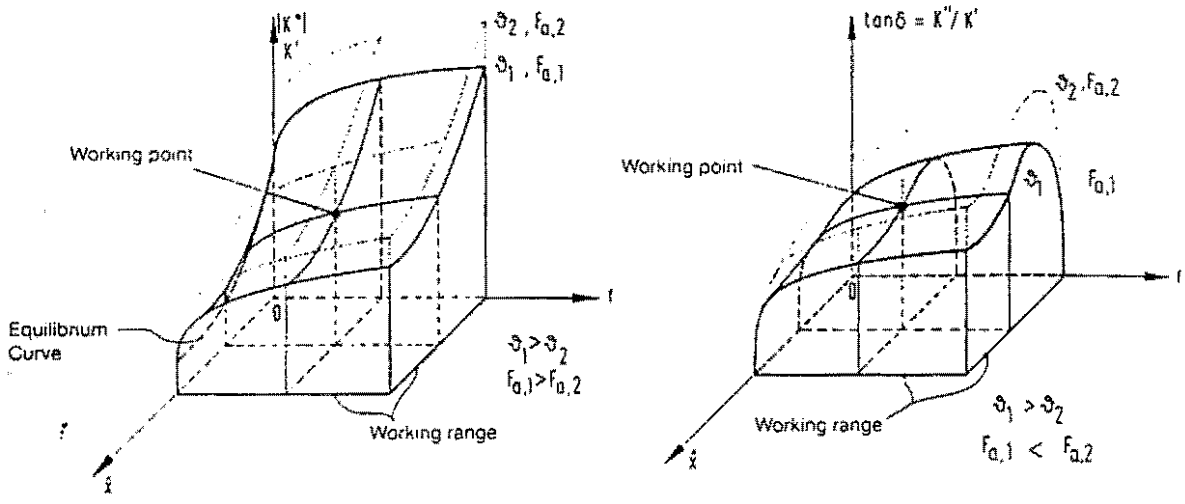

Figure 12: Performance Graphs for Spring Rate and Loss Coefficient

Two measured hysteretic loops at different frequencies are given in figure 13. The strong dependency of the investigated high damping materials on the dynamic amplitude is demonstrated in figure 14.

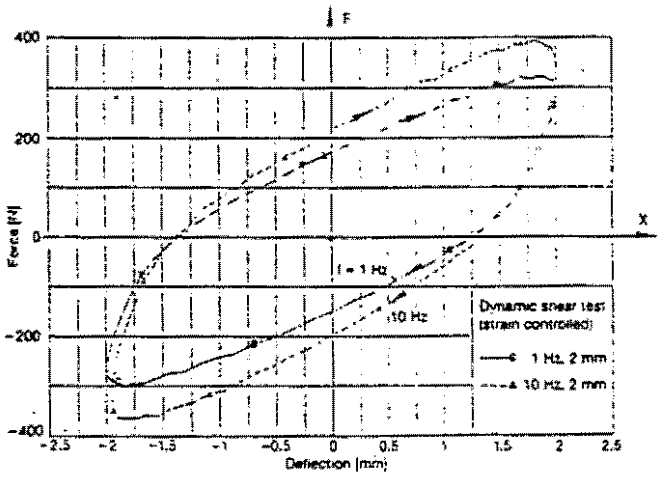

Figure 13: Hysteretic Loops as a Function of Frequency f

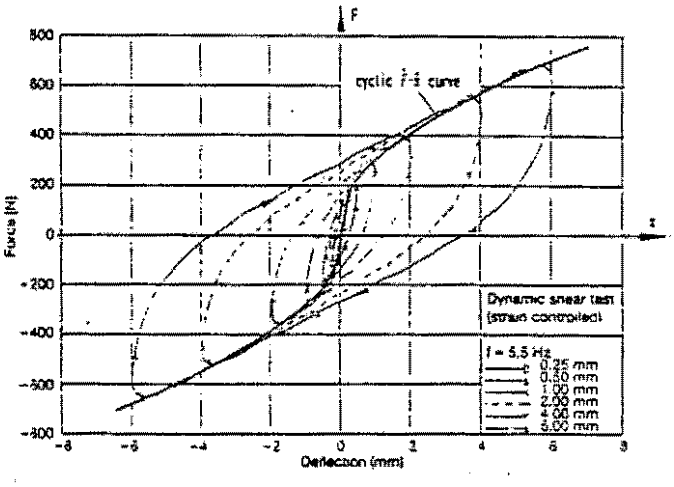

Figure 14: Hysteretic Loops as a Function of Amplitude $\hat{x}$

Figure 15 shows in a qualitative manner the typical temperature characteristic of high damping elastomers.

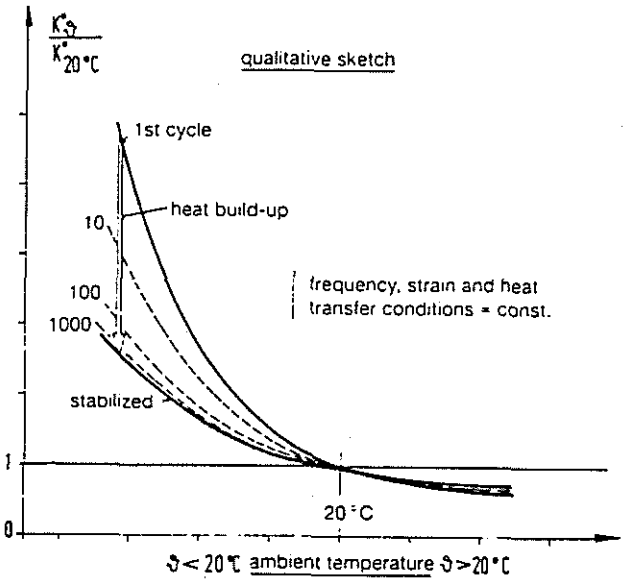

Figure 15: Dynamic Stiffness as a Function of Ambient Temperature and Heat build-up

The vibration response and the dissipation characteristic of viscoelastic dampers under double-frequency input excitation have been analytically and experimentally investigated.
An example is shown in figure 16. Various test results show good agreement between measured and theoretical response data.

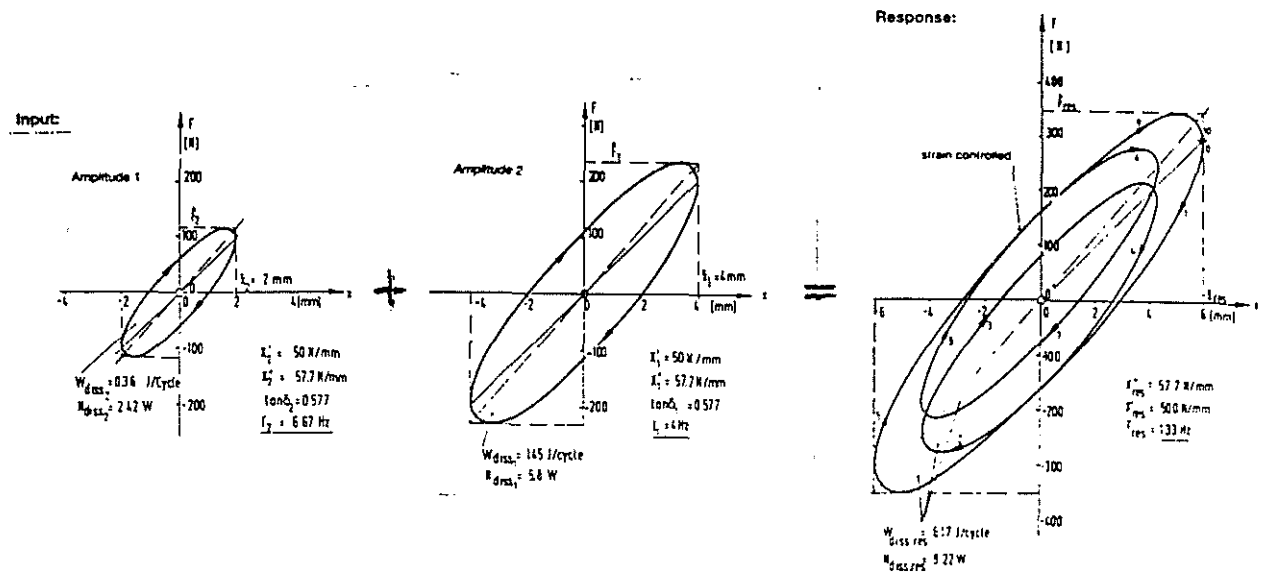

Figure 16: Multifrequency Response (Calculated Result, Silicone Rubber)

The most frequently used representation of the damper characteristic in the time domain is given by the linear differential equation form:

$$F + P_1 \dot{F} + P_2 \ddot{F} + P_3 \dddot{F} + \ldots + P_{(n)} F^{(n)} = K_e x + Q_1 \dot{x} + Q_2 \ddot{x} + \ldots + Q_{(m)} x^{(m)}$$

where $(\,)^{\cdot} = d/dt$.

It is possible to transform this equation into the frequency domain by means of integral transformations. The damper identification parameters P, Q, K_e can be determined in the frequency domain and then be transformed back.

6. Determination of Material Parameters

6.1 Hyperelastic Material Behavior

Most of elastomer materials can be described in the equilibrium state by means of can hyperelastic constitutive equation. The mechanical properties of these Green-elastic materials are characterized by the strain energy function (hyper-elastic potential):

$W = W(I_B, II_B, III_B)$, dependent on the 3 invariants of the left Cauchy-Green deformation tensor.

For an incompressible material is ($III_B = 1$) and (W) depends only on the two deformation invariants, (I_B) and (II_B).
This strain energy density function can be approximated by a power series expansion of (I_B-3) and (II_B-3):

$$W(I_B, II_B) = \sum_{i,j}^{k,l} C_{ij} \cdot (I_B - 3)^i \cdot (II_B - 3)^j = W(C_{ij})$$

The coefficients C_{10}, C_{01}, C_{11}, C_{20}, C_{02}, ... are material constants which are obtained from experimental data.
The constitutive equations for an incompressible material can be written in the following form:

$$\bar{\sigma}_{ij} = 2 \cdot \left[(G_{ij}) \left(\frac{\partial W}{\partial I_B} \right) - (G_{ij})^{-1} \left(\frac{\partial W}{\partial II_B} \right) \right] - P\delta_{ij}$$

where: P = arbitrary pressure, δ_{ij} = 'Kronecker delta'

G_{ij} (G_{ij}^{-1}) = right (inverse) Cauchy-Green deformation tensor.

$\bar{\sigma}_{ij}$ = Cauchy-stress tensor (true stress).

The equations, derived from the expansion of the strain energy density, are linear in the coefficients, C_{ij}. Therefore, they can be obtained by least squares fitting of experimental data on a computer. For example, figure 17 represents the determination of hyperelastic material parameters (Signorini-potential) from tension and compression tests.

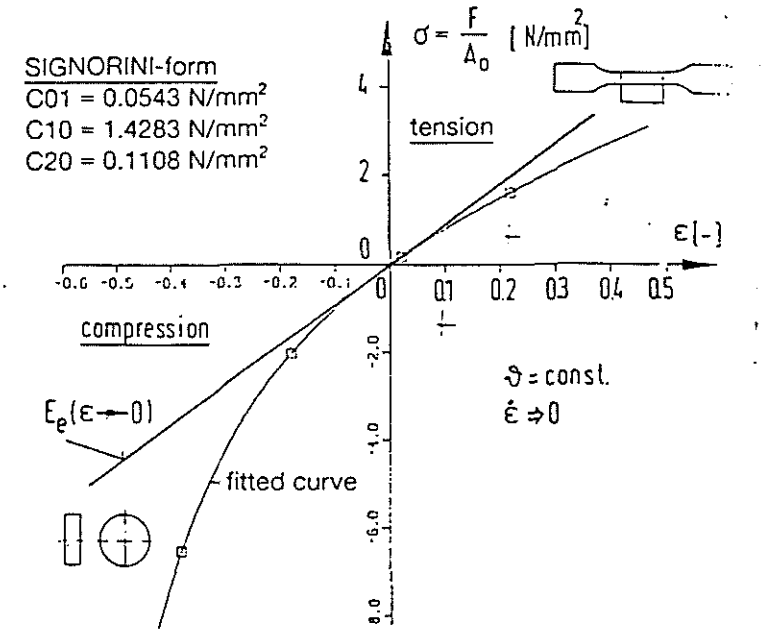

Figure 17: Determination of Hyperelastic Material Coefficients

6.2 Viscoelastic Material Behavior

The usual frequency-domain formulation of the three-dimensional viscoelastic constitutive equation can be expressed by

$$S_{ij}^*(i\omega) = 2G^*(i\omega)\, e_{ij}^* = 2\cdot(G' + i\cdot G'')\, e_{ij}^* \quad \text{(dilatation)}$$

and $$\sigma_{ii}^*(i\omega) = 3B^*(i\omega)\, \varepsilon_{ii}^* = 3\cdot(B' + i\cdot B'')\, \varepsilon_{ii}^* \quad \text{(distortion)}$$

where S_{ij}^*, (e_{ij}^*) : complex stress (strain) tensor deviator, $\gamma_{ij}^* = 2e_{ij}^*$

σ_{ii}^*, (ε_{ii}^*) : trace of the stress (strain) tensor

G^*, (B^*) : complex shear (bulk) modulus

The complex shear modulus is defined as

$$G^*(i\omega) = \tau^*/\gamma^* = G' + i \cdot G'' = G_e + \mathbf{h}^*(i\omega)$$

where G_e: equilibrium shear modulus, $\mathbf{h}^*(i\omega)$: dissipation function.
Based on a linear dissipation function, the complex shear modulus can be approximated by

$$G^*(i\omega) = \frac{G_e + (i\omega)q_1 + (i\omega)^2 q_2 + (i\omega)^3 q_3 + \ldots + (i\omega)^m q_m}{1 + (i\omega)p_1 + (i\omega)^2 p_2 + (i\omega)^3 p_3 + \ldots + (i\omega)^n p_n} = G' + iG''$$

The viscoelastic material coefficients G_e, q_i, p_i can be obtained by fitting the nonlinear equations $G'(\omega)$, $G''(\omega)$ or $G^*(\omega)$, $\eta(\omega)$ to measured curves by means of appropriate numerical methods (least-squares fitting a.o.). These material parameters correspond to those in the following differential equation of the time domain (equivalent form): ($s_{ij} \triangleq \tau_{ij}$)

$$\tau_{ij} + p_1 \dot{\tau}_{ij} + p_2 \ddot{\tau}_{ij} + \ldots + p_n \overset{(n)}{\tau}_{ij} = G_e \cdot \gamma_{ij} + q_1 \dot{\gamma}_{ij} + q_2 \ddot{\gamma}_{ij} + \ldots + q_m \overset{(m)}{\gamma}_{ij}$$

Figure 18 shows the approximation of measured storage modulus $G'(\omega)$ and loss modulus $G''(\omega)$ by means of models of a different number of parameters:

o 4-parameter-model:

$$\tau + p_1 \dot{\tau} = G_e \cdot \gamma + q_1 \dot{\gamma} + q_2 \ddot{\gamma}$$

o 10-parameter-model:

$$\tau + p_1 \dot{\tau} + p_2 \ddot{\tau} + p_3 \dddot{\tau} + p_4 \ddddot{\tau} = G_e \cdot \gamma + q_1 \dot{\gamma} + q_2 \ddot{\gamma} + q_3 \dddot{\gamma} + q_4 \ddddot{\gamma} + q_5 \overset{\bullet\bullet\bullet\bullet\bullet}{\gamma}$$

The dynamic characteristic for the total frequency range can be represented by means of the polar frequency response locus for a particular dynamic shear strain γ (figure 19).

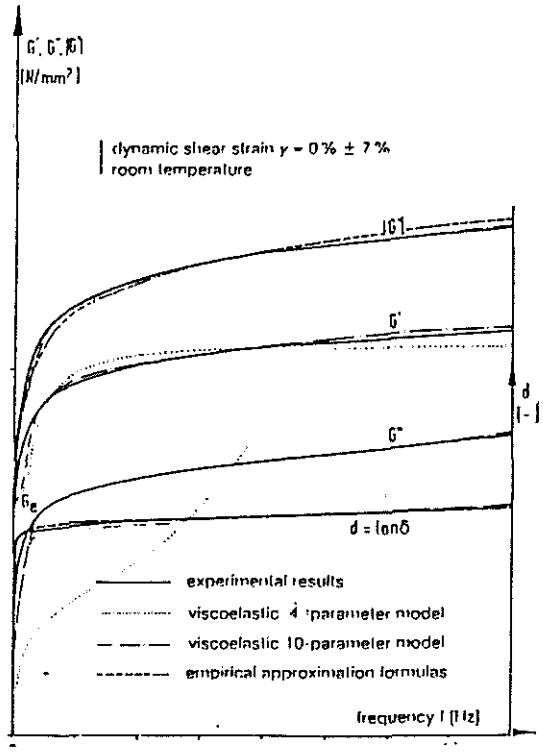

Figure 18: Storage Modulus and Loss Modulus as a Function of Frequency

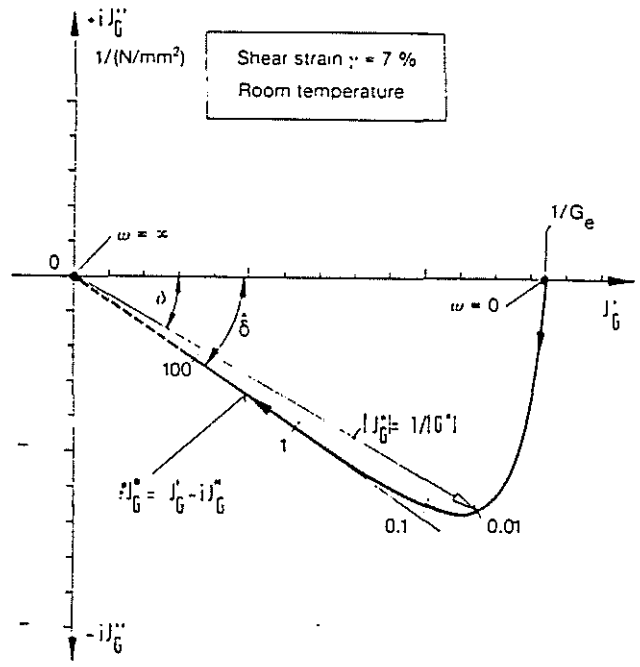

Figure 19: Polar Frequency Response Locus of a Viscoelastic Damper Material (J^*_G Complex Compliance)

Non-linearities of the dynamic stress-strain behaviour arise from two sources:

- modes of deformation and geometries
- inherent nonlinearities due to material behaviour

In the second case, the material coefficients are dependent on amplitude, temperature etc. Figures 20 and 21 show an example of the influence of shear strain on the dynamic modulus and the loss factor at a constant frequency.

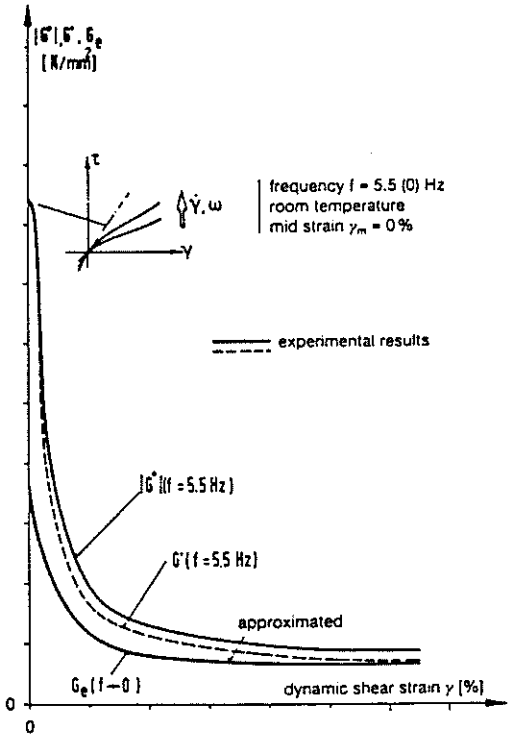

Figure 20: Dynamic and Static Modulus as a Function of Shear Strain

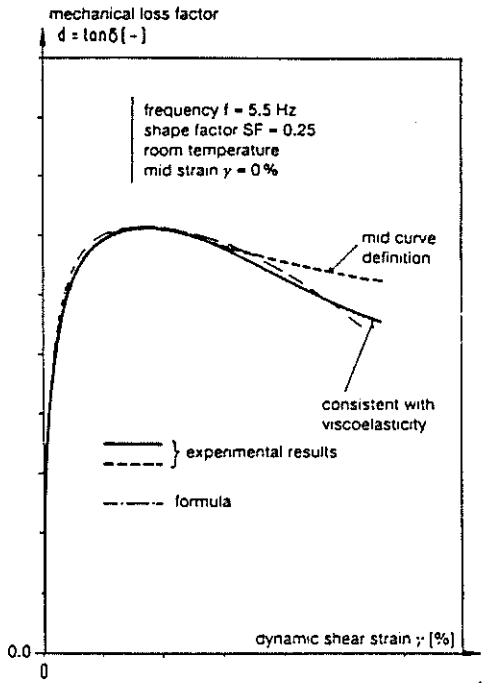

Figure 21: Mechanical Loss Factor as a Function of Shear Strain

Alternatively, the equivalent convolution integral equation can used for the description of isotrope linearized viscoelastic materials; for example:

$$S_{ij}(t) = 2 \cdot e_{ij}(0) \cdot G_R(t) + 2 \cdot \int_0^t G_R(t-\tau) \cdot \frac{de_{ij}}{d\tau} \, d\tau$$

(relaxation integral form)

In the time domain, the relaxation (creep) modulus is experimentally determined by means of uniaxial relaxation (creep) tests. The relaxation modulus $G_R(t)$ can, for example, be approximated by the finite Prony-Dirichlet series:

$$G_R(t) = G_e + \hat{G}(t) = G_e + \sum_{i=1}^{k} G_i \cdot e^{-t/\tau_i}$$

For a given relaxation experiment, the material parameters can be computed by using least-squares techniques or a simple collocation. These material parameters are related to all other material coefficients in the time and frequency domain.
Figure 22 represents this fitting method by means of an uniaxial tension-relaxation test. The selected Prony-Dirichlet serie (k = 7), shows good agreement with experimental data.

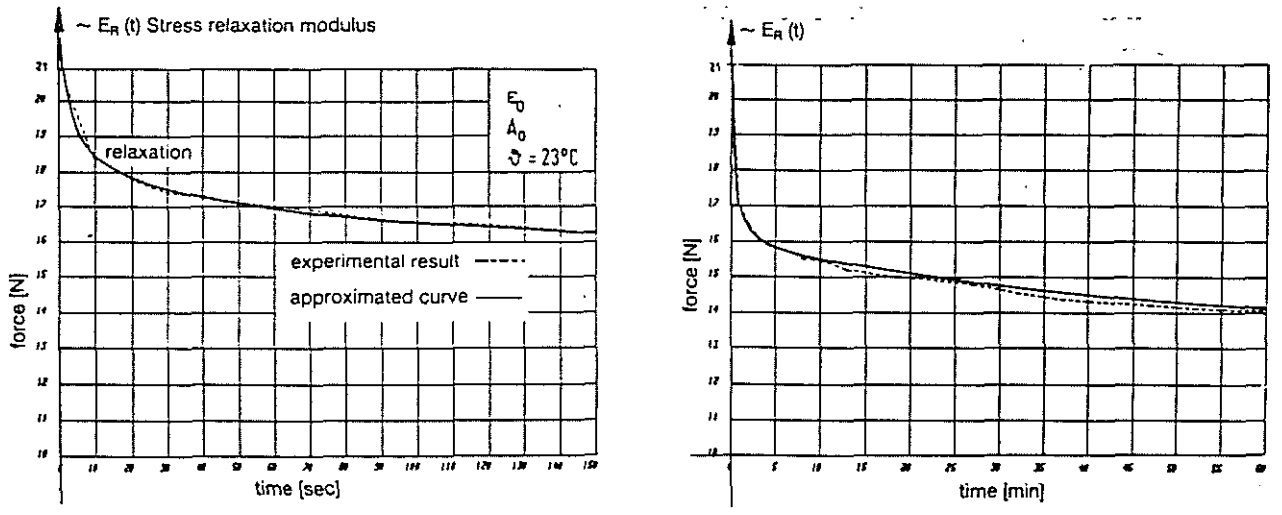

Figure 22: Determination of the Viscoelastic Material Parameters from a Relaxation Test

In addition figure 23 represents an uniaxial creep-tension test and its numerical approximation (k = 7).

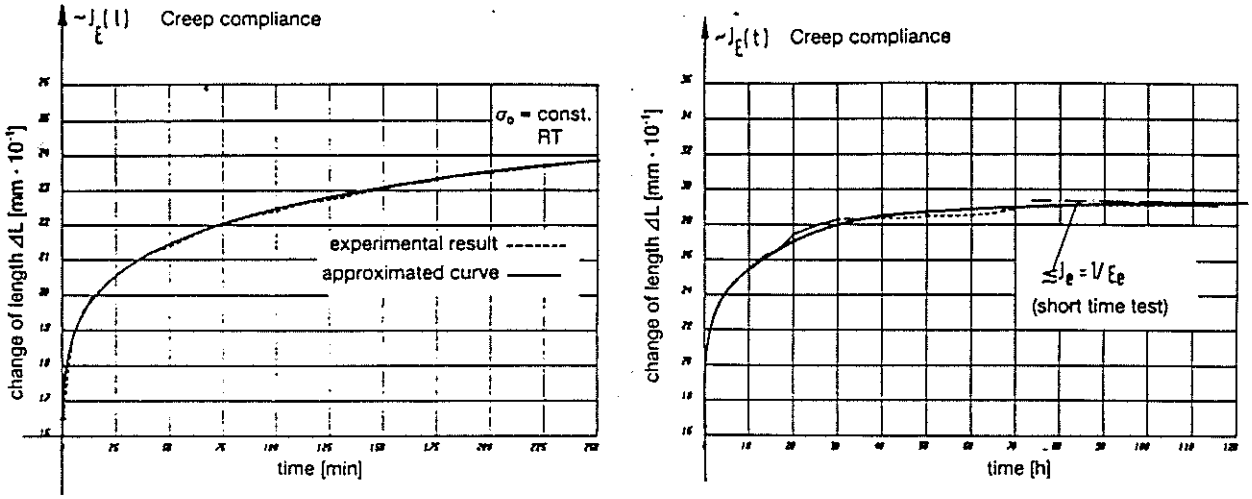

Figure 23: Determination of the Viscoelastic Material Parameters from a Creep Test

Conclusions

Optimization of viscoelastic dampers requires an accurate knowledge of spring rates, strength and dissipation characteristic at varios load and environmental conditions.
This paper presents experimental and theoretical results on the identification and analysis of elastomeric lead-lag dampers in terms of appropriate model constants.
The determined nonlinear-elastic and viscoelastic material coefficients are the base for the calculation of spring rates, loss power, strain- and temperature distributions.

References

[1] DIN 53513
Bestimmung der visko-elastischen Eigenschaften von Elastomeren

[2] ISO 4664
Rubber-Determination of dynamic properties of vulcanization for classification purposes (by forced sinusoidal shear strain)

[3] ISO 2856 Elastomer-General requirements for dynamic testing

[4] A.D. Nashif, D.I.G. Jones, J.P. Henderson
Vibration Damping
J.Wiley & Sons, New York (1985)

[5] J.D. Ferry
Viscoelastic Properties of Polymers
J.Wiley & Sons, New York (1970)

[6] J.C. Snowdon
Vibration and Shock in Damped Mechanical Systems
J.Wiley & Sons, New York (1968)

[7] R.M. Christensen
Theory of Viscoelasticity
Academic Press, New York (1971)

[8] Wilhelm Flügge
Viscoelasticity (Second edition)
Springer, Berlin (1975)

[9] R.W. Ogden
Non-Linear Elastic Deformations
ELLIS HORWOOD LIM. (1984)